The Journal of Neuroscience, September 15, 1998, *18*(18):7152–7159

Central $P2X_4$ and $P2X_6$ Channel Subunits Coassemble into a Novel Heteromeric ATP Receptor

Khanh-Tuoc Lê, Kazimierz Babinski, and Philippe Séguéla

Cell Biology of Excitable Tissue Group, Montreal Neurological Institute, McGill University, Montreal, Quebec, Canada H3A 2B4

Ionotropic ATP receptors are widely expressed in mammalian CNS. Despite extensive functional characterization of neuronal homomeric P2X receptors in heterologous expression systems, the subunit composition of native central P2X ATP-gated channels remains to be elucidated. $P2X_4$ and $P2X_6$ are major central subunits with highly overlapping mRNA distribution at both regional and cellular levels. When expressed alone in *Xenopus* oocytes, $P2X_6$ subunits do not assemble into surface receptors responsive to ATP applications. On the other hand, $P2X_4$ subunits assemble into bona fide ATP-gated channels, slowly desensitizing and weakly sensitive to the partial agonist α,β-methylene ATP and to noncompetitive antagonists suramin and pyridoxal-5-phosphate-6-azophenyl-2′,4′-disulfonic acid. We demonstrate here that the coexpression of $P2X_4$ and $P2X_6$ subunits in *Xenopus* oocytes leads to the generation of a novel pharmacological phenotype of ionotropic ATP receptors. Heteromeric $P2X_{4+6}$ receptors are activated by low-micromolar α,β-methylene ATP ($EC_{50} = 12\ \mu M$) and are blocked by suramin and by Reactive Blue 2, which has the property, at low concentrations, to potentiate homomeric $P2X_4$ receptors. The assembly of $P2X_4$ with $P2X_6$ subunits results from subunit-dependent interactions, as shown by their specific copurification from HEK-293 cells transiently transfected with various epitope-tagged P2X channel subunits. Our data strongly suggest that the numerous cases of neuronal colocalizations of $P2X_4$ and $P2X_6$ subunits observed in mammalian CNS reflect the native expression of heteromeric $P2X_{4+6}$ channels with unique functional properties.

Key words: purinoceptor; nucleotide; transmitter-gated cation channel; α,β methylene ATP; suramin; PPADS

Fast purinergic neurotransmission is mediated by nonselective cation channels gated by extracellular ATP. These transduction proteins, designated P2X receptors, constitute a distinct class of neurotransmitter-gated channels on the basis of their primary cDNA sequences and their predicted transmembrane protein topology. Currently, seven mammalian P2X genes have been identified with either expression or homology cloning assays (Buell et al., 1996). Among the neuronal P2X receptors, only $P2X_4$ and $P2X_6$ isoforms are predominantly expressed in the adult rat brain in which they show an overlapping pattern of regional and cellular distribution at the mRNA level (Collo et al., 1996). Homomeric rat $P2X_4$ receptors expressed in HEK-293A cells or *Xenopus laevis* oocytes and homomeric $P2X_6$ receptors silent in oocytes (Soto et al., 1996) but functional in HEK-293A cells (Collo et al., 1996) are weakly responsive to α,β-methylene ATP ($\alpha\beta$mATP) and to P2 antagonists suramin and pyridoxal-5-phosphate-6-azophenyl-2′,4′-disulfonic acid (PPADS) (North and Barnard, 1997). Yet, native ionotropic purinergic responses from rat medial habenula, cerebellum, and hippocampus were blocked by P2 antagonists, and most native ATP receptors are activated by $\alpha\beta$mATP (Edwards et al., 1992; Mateo et al., 1998; Ross et al., 1998). Moreover, high-affinity [^{3}H]$\alpha\beta$mATP autoradiographic binding sites have been localized in specific but widespread regions within the brain and spinal cord (Bo and Burnstock, 1994; Michel and Humphrey, 1994; Balcar et al., 1995). Discrepancies between pharmacological profiles of heterologously expressed homo-oligomeric P2X subunits and electrophysiological recordings from neuronal preparations likely reflect the existence of native heteromeric phenotypes of P2X receptors in peripheral nervous system as well as the CNS. Indeed, one such hybrid P2X phenotype was recorded in sensory neurons (Khakh et al., 1995; Lewis et al., 1995) and has been proposed to result from the association between coexpressed $P2X_2$ and $P2X_3$ subunits (Chen et al., 1995; Lewis et al., 1995; Radford et al., 1997). We describe in this report a novel P2X heteromeric receptor containing central $P2X_4$ and $P2X_6$ subunits. This phenotype of ATP-gated channel is endowed with a unique pharmacology characterized by increased sensitivities to $\alpha\beta$mATP, 2-methylthio-ATP (2MeSATP), suramin, PPADS, and Reactive Blue 2 (RB-2) in *Xenopus* oocytes.

MATERIALS AND METHODS

Molecular biology. Wild-type full-length $P2X_6$ subunit cDNA was obtained by RT-PCR using adult rat spinal cord RT-cDNA template, Expand DNA polymerase (Boehringer Mannheim, Indianapolis, IN), and exact match primers based on published primary sequences (Collo et al., 1996; Soto et al., 1996). Construction of $P2X_1$-Flag and $P2X_4$-Flag was reported previously (Lê et al., 1998). To generate epitope-tagged $P2X_6$-Flag and $P2X_4$-$(His)_6$ subunits, an *Xho*I–*Xba*I cassette containing an in-frame His_6 epitope followed by an artificial stop codon was grafted to the full-length *Hin*dIII–*Xho*I $P2X_4$ construct. The $P2X_4$-$(His)_6$ mutant was then subcloned directionally into the *Hin*dIII and *Xba*I sites of pcDNAI vector (Invitrogen, San Diego, CA) for cytomegalovirus-driven heterologous expression in mammalian cells and *Xenopus laevis* oocytes. Epitope-tagged and RT-PCR constructs were subjected to dideoxy sequencing either manually with Sequenase (Upstate Biotechnology,

Received April 6, 1998; revised June 22, 1998; accepted July 6, 1998.

K-T.L. holds a PhD studentship from the Savoy Foundation for Epilepsy; K.B. is a Medical Research Council-PMAC-Astra postdoctoral Fellow; and P.S. is a junior Scholar from the Fonds de la Recherche en Santé du Québec. We thank the Medical Research Council of Canada, the Fondation des Maladies du Coeur du Québec, and the Astra Research Center in Montreal for their operating support, as well as Michel Paquet for expert technical assistance.

Correspondence should be addressed to Dr. Philippe Séguéla, Cell Biology of Excitable Tissue Group, Montreal Neurological Institute, 3801 University Avenue, Room 778, Montreal, Quebec, Canada H3A 2B4.

Lake Placid, NY) or with an ALF DNA sequencer (Pharmacia, Piscataway, NJ).

Cell culture and protein chemistry. For cDNA transfections of epitope-tagged and wild-type P2X subunits into mammalian cells, HEK-293A cells (CRL 1573; American Type Culture Collection, Rockville, MD) were cultured in DMEM and 10% heat-inactivated fetal bovine serum (FBS) (Wisent, St-Bruno, Quebec, Canada) containing penicillin and streptomycin. Freshly plated cells reaching 30–50% confluency were used for transient cDNA transfections with the calcium phosphate method on 90 mm cell culture dishes (Falcon) with 10 μg of supercoiled plasmid cDNA/10^6 cells (Lê et al., 1998). For Western blots, transfected HEK-293A cells were lifted in Hank's modified calcium-free medium with 20 mM EDTA, pelleted at low centrifugation, and homogenized in 10 volumes of 10 mM HEPES buffer, pH 7.4, containing protease inhibitors phenylmethylsulfonyl fluoride (0.2 mM) and benzamidine (1 mM). Cell lysates were pelleted at 14,000 × *g* for 5 min, and membrane proteins in supernatants were solubilized with SDS-containing loading buffer. Approximately 150 μg of protein/lane were run on 12% SDS-PAGE and then transferred to nitrocellulose. Immunoprobing was performed with mouse mAb M2 (1 μg/ml, IBI) followed by peroxidase-labeled anti-mouse secondary antibodies for visualization by enhanced chemiluminescence (Amersham, Oakville, Ontario, Canada). Copurification of associated P2X subunits was performed as previously described for IRK channels (Tinker et al., 1996) with minor modifications. Cell lysates were solubilized with 5% Triton X-100 for 2 hr at 4°C. Unsolubilized materials were pelleted at 10,000 × *g*, and supernatants were incubated with 50 μl of 50% slurry of equilibrated Ni-NTA-Resin (Qiagen, Hilden, Germany) for 2 hr at 4°C. Nickel beads were then washed six times in TBS containing 25 mM imidazole and 1% Triton X-100. Bound proteins were eluted from Ni-NTA resin with 500 mM imidazole, diluted 1:1 (v/v) with SDS-containing loading buffer, and warmed for 10 min at 37°C. Samples were then loaded onto a 12% SDS-PAGE, transferred to nitrocellulose, and analyzed in Western blot using chemiluminescence as above.

Electrophysiology. For electrophysiological recordings in oocytes, ovary lobes were surgically removed from *Xenopus laevis* frogs anesthetized with Tricaine (Sigma, St. Louis, MO) and treated for 3 hr at room temperature with type II collagenase (Life Technologies, Gaithersburg, MD) in calcium-free Barth's solution under vigorous agitations. Stage V–VI oocytes were then defolliculated chemically before nuclear microinjections of 5–10 ng of cDNA coding for each P2X channel subunit. After 2–5 d of incubation at 19°C in Barth's solution containing 1.8 mM calcium chloride ($CaCl_2$) and 10 μg/ml gentamicin, P2X currents were recorded in a two-electrode voltage-clamp configuration using an OC-725B amplifier (Warner Institute). Signals were low-pass-filtered at 1 kHz, acquired at 500 Hz using a Macintosh IIci equipped with an NB-MIO-16XL analog-to-digital card (National Instruments). Traces were postfiltered at 100 Hz in Axograph (Axon Instruments). Agonists, antagonists, and cofactors (zinc chloride, pH 6.5 and 8.0) were dissolved in Ringer's solution containing (in mM): 115 NaCl, 2.5 KCl, and 1.8 $CaCl_2$ in 10 HEPES, pH 7.4 standard at room temperature, and applied on oocytes at a constant flow rate of 12 ml/min. Dose–response curves and EC_{50} values were derived from fittings for the sigmoidal equation of Hill using Prism 2.0 software (Graphpad Software, San Diego, CA).

Statistical analysis. All comparisons involving two variances were performed with Fisher's *F* values (variance homogeneity requirements) and with Student's *t* tests for two unpaired groups. Two-tailed statistical thresholds, for both Fisher's *F* and Student's *t* critical values, were set at $p < 0.05$.

RESULTS

Functional impact of $P2X_6$ subunit expression on ATP-induced currents

In response to 100 μM ATP, *Xenopus* oocytes microinjected with a mix of $P2X_4$ and $P2X_6$ cDNAs (1:1 molar ratio) gave rise to currents with kinetic profiles similar to those observed with oocytes expressing $P2X_4$ alone (Fig. 1*A*). $P2X_6$ by itself appeared to be silent in *Xenopus* oocytes, because no current was detected during ATP applications (Fig. 1*A*), in agreement with what has been reported previously (Soto et al., 1996). Comparison of peak current amplitudes after 3 d of expression revealed, however, that currents from cells coexpressing $P2X_4$ and $P2X_6$ subunits were reproducibly and significantly smaller than currents from cells expressing only $P2X_4$ receptors (Fig. 1*A,B*), suggesting the possibility that the $P2X_6$ channel subunit can heteropolymerize with other members of the P2X family. We coexpressed $P2X_6$ together with $P2X_1$ (Valera et al., 1994) or with $P2X_2$ (Brake et al., 1994). In response to 100 μM ATP, there were no differences between peak currents recorded from oocytes coexpressing $P2X_1$ and $P2X_6$ and those expressing $P2X_1$ alone (Fig. 1*C*) after 3 d of expression. Similarly, we did not observe any functional impact of $P2X_6$ on the expression of $P2X_2$ under the same experimental conditions (Fig. 1*D*), eliminating the possibility of a general inhibitory effect of $P2X_6$ on protein synthesis or on translocation. Thus these data indicate either that the subunit-specific interaction between $P2X_4$ and $P2X_6$ isoforms generates a heteromeric $P2X_{4+6}$ receptor, or that $P2X_6$ subunits exert a specific inhibitory function on $P2X_4$ receptor expression. If $P2X_{4+6}$ heteromers are expressed, smaller peak currents could result from a lower affinity for ATP or a smaller single conductance in comparison with homomeric $P2X_4$ channels. Alternatively, smaller ATP responses at day 3 could simply reflect a slower kinetics of receptor expression.

To further characterize a time-dependent effect, we studied the time course of expression, daily recording peak currents in response to 100 μM ATP from oocytes expressing either $P2X_4$ and $P2X_6$ cDNAs or $P2X_4$ cDNA alone. Figure 2 demonstrates that ATP receptors in oocytes coexpressing $P2X_4$ and $P2X_6$ subunits, compared with $P2X_4$ alone, needed a longer time to reach the same levels of ATP-induced currents. However, between days 2 and 5 after injection, there was a dramatic sevenfold increase in peak current amplitudes in oocytes coexpressing $P2X_4$ and $P2X_6$ subunits (Fig. 2*A*). This profile is in striking contrast with the time course of $P2X_4$ expression that slowly decayed over the same period (Fig. 2*B*).

Agonist sensitivity profile of $P2X_{4+6}$ heteromeric receptors

No significant difference was detected between the EC_{50} values derived from ATP dose–response profiles of $P2X_{4+6}$ (6.3 ± 0.9 μM) channel phenotype and homomeric $P2X_4$ (4.2 ± 1.1 μM) receptors (Fig. 3*A*) expressed in oocytes. However, the partial agonist 2MeSATP had EC_{50} values of 7.67 ± 1.01 and 26 ± 1.8 μM for $P2X_{4+6}$ and $P2X_4$ receptors, respectively, a statistically significant difference (Fig. 3*B*). Even more striking, in response to 100 μM αβmATP on day 3 after injection, oocytes expressing $P2X_{4+6}$ heteromeric channels gave rise to peak current amplitudes of 0.7 ± 0.13 μA compared with 0.12 ± 0.02 μA only from oocytes expressing $P2X_4$ homomeric receptors, in marked contrast with the situation observed in response to ATP (compare Figs. 4A, 1*B*). The αβmATP EC_{50} values were found to be 12 ± 2 μM for $P2X_{4+6}$ and 55 ± 2 μM for $P2X_4$ channel phenotypes (Fig. 4*B*). Therefore, αβmATP shows more potency and has a higher affinity on $P2X_{4+6}$ receptors than on $P2X_4$ receptors. These different sensitivities to 2MeSATP and αβmATP constitute more experimental evidence for a functional association between $P2X_4$ and $P2X_6$ subunits coexpressed in *Xenopus* oocytes.

Sensitivity of $P2X_{4+6}$ receptors to suramin, PPADS, and RB-2

It is widely recognized that neither $P2X_4$ nor $P2X_6$ homomeric receptors (in HEK-293 cells) are completely blocked by suramin or PPADS up to 100 μM without preincubation (Buell et al., 1996; Collo et al., 1996). In response to 100 μM ATP and 10 μM suramin coapplications without preincubation, oocytes expressing $P2X_{4+6}$

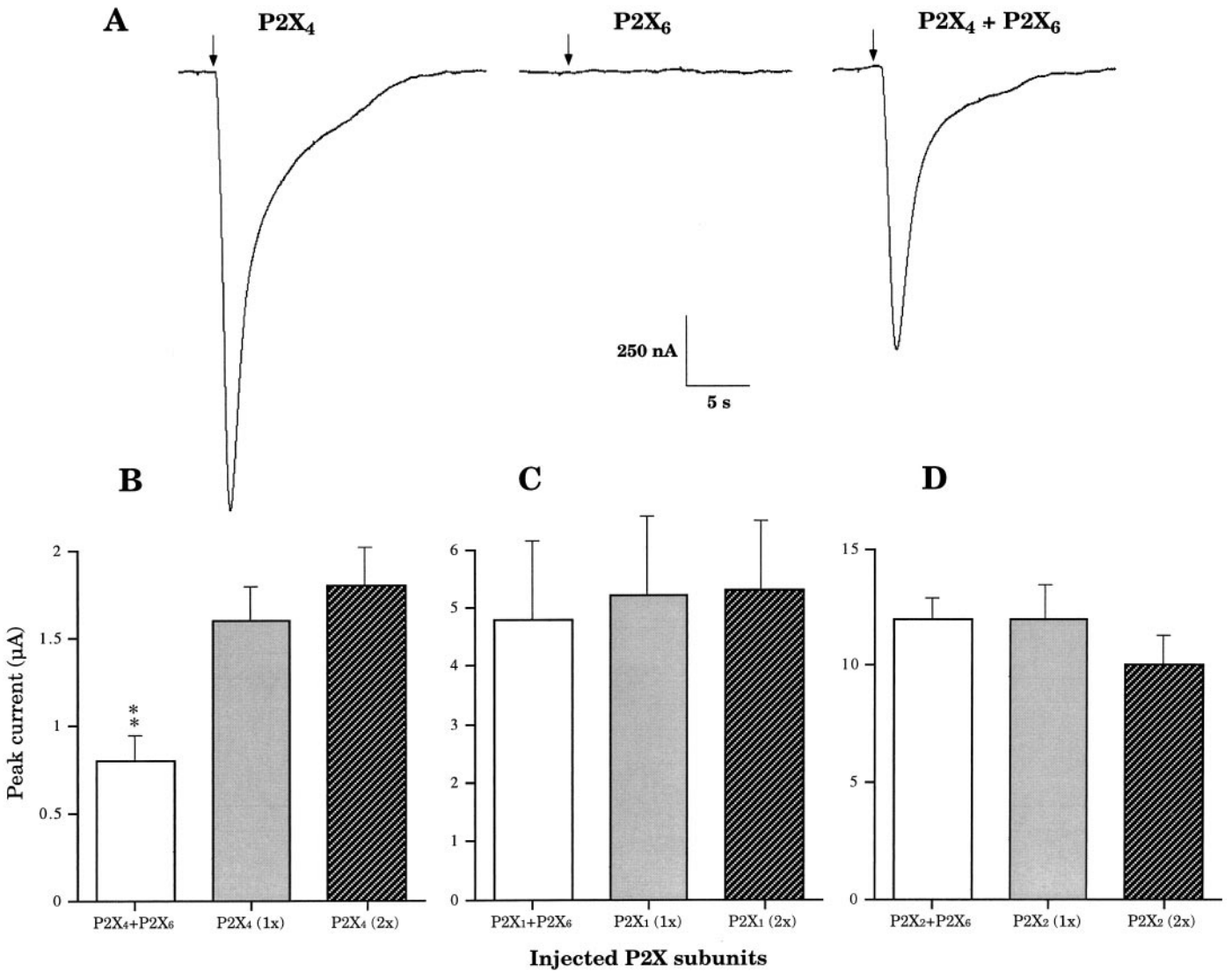

Figure 1. Representative heteromeric $P2X_{4+6}$ channel current phenotype at day 3. *A*, ATP-induced currents after heterologous expression of $P2X_4$, $P2X_6$, and $P2X_4$ + $P2X_6$ (1:1 molar ratio) subunits recorded 3 d after corresponding cDNA nuclear microinjections in *Xenopus* oocytes. *Arrows* indicate beginnings of ATP applications (10 sec). *B*, $P2X_4$-dependent functional impact of $P2X_6$ on ATP-induced response ($P2X_4$ expressed alone; *1x*, 5 ng of cDNA; *2x*, 10 ng). *C*, $P2X_1$ receptor ($P2X_1$; *1x*, 5 ng; *2x*, 10 ng) functional expression is unaffected by coexpressed $P2X_6$ subunits. *D*, $P2X_2$-mediated ($P2X_2$; *1x*, 5 ng; *2x*, 10 ng) ATP-induced peak current amplitudes are unchanged in the presence of $P2X_6$ subunits. (Averages ± SEM from 3 to 15 oocytes in 2–4 independent experiments; double asterisks denote significant difference; $p < 0.01$).

gave rise to residual currents of 61 ± 3% (Fig. 5) of the response to 100 μM ATP (100%). Under the same experimental conditions, oocytes expressing $P2X_4$ receptors alone were almost unaffected (93 ± 3%; Fig. 5). We have also found that 10 μM PPADS coapplied with 100 μM ATP gave rise to peak current amplitudes of 83 ± 7 and 103 ± 6% for $P2X_{4+6}$ and $P2X_4$ receptor phenotypes, respectively (Fig. 5*B*), but we did not find any significant difference between this 17% inhibition on $P2X_{4+6}$ and no effect on $P2X_4$. We have also investigated the effects of RB-2 by coapplying 10 μM of the antagonist with 100 μM ATP: oocytes expressing $P2X_{4+6}$ receptor phenotypes were characterized by residual peak currents of 60 ± 9% compared with potentiated peak currents of 123 ± 18% from oocytes expressing $P2X_4$ receptors alone (Fig. 5*A*). Preincubation of the cell with antagonist during 1 min before coapplication with ATP resulted in even more dramatic phenotypical differences between $P2X_4$ and $P2X_{4+6}$ for suramin (23% blockade vs 41%) and PPADS (19% blockade vs 38%) (Fig. 5*B*). Furthermore, in conditions of preincubation, 10 μM RB-2 blocked $P2X_{4+6}$ heteromeric channels by up to 26% but increased $P2X_4$ response by >45% (Fig. 5*B*). A potentiating effect of RB-2 on $P2X_4$ homomeric receptors has been reported in oocytes, albeit to a smaller extent (Bo et al., 1995).

Sensitivity of $P2X_{4+6}$ receptors to coagonists zinc ions and protons

We have reported previously that 10 μM extracellular zinc ions coapplied with 10 μM ATP potentiated $P2X_4$ peak currents by almost twofold (Séguéla et al., 1996). In addition, it has also been shown that the sensitivity to ATP of homomeric $P2X_4$ channels is modulated by external pH: pH <7 inhibits ATP responses, whereas pH >8 has no significant effects (Stoop et al., 1997). Therefore, we checked whether these coagonists applied with ATP could discriminate between $P2X_{4+6}$ and $P2X_4$ receptor phenotypes. In response to 10 μM zinc ions and 10 μM ATP

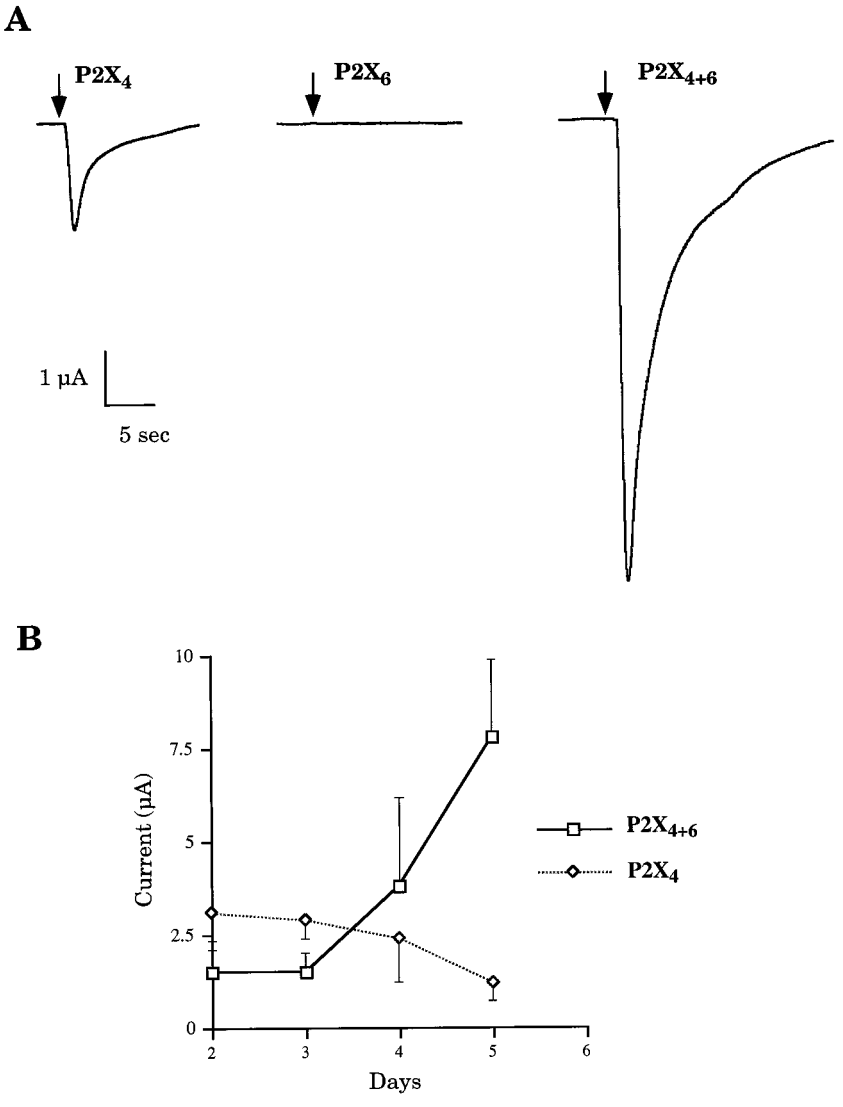

Figure 2. *A*, Potentiation of ATP response represented by $P2X_{4+6}$ channel current phenotype at day 5. *Arrows* indicate beginnings of ATP applications (10 sec). *B*, Time course of heteromeric $P2X_{4+6}$ expression. Kinetics of appearance of functional ATP receptors on plasma membranes is strikingly different in oocytes coinjected with $P2X_4$ and $P2X_6$ subunits compared with those injected with $P2X_4$ subunits (averages ± SEM from 3 to 15 oocytes in 2–8 independent experiments).

coapplications, there were no significant differences between potentiating factors of 1.8 ± 0.19 and 1.8 ± 0.21 for $P2X_{4+6}$ heteromeric channels and $P2X_4$ homomeric receptors, respectively (Fig. 6*A*). There was also no significant difference between these two receptor phenotypes with respect to ATP (20 μM) applied at pH 6.5. In both cases, residual peak current amplitudes were 46 ± 4% of control values measured at pH 7.4 (Fig. 6*B*). When 20 μM ATP was applied at pH 8.0, it elicited peak currents of 121 ± 4 and 106 ± 4% for $P2X_{4+6}$ heteromers and $P2X_4$ homomers, respectively (Fig. 6*C*). Thus, contrary to αβmATP, 2MeSATP, and antagonists suramin, PPADS, and RB-2, cofactors zinc and protons did not discriminate between $P2X_{4+6}$ and $P2X_4$ receptors on a pharmacological basis.

Subunit-specific association of $P2X_4$ with $P2X_6$ subunits

Before testing their biochemical interaction, the expression of Flag-tagged $P2X_1$, $P2X_4$, and $P2X_6$ subunit proteins in transiently transfected HEK-293A cells was confirmed by immunoblot of total membrane proteins (Fig. 7*A*, *lanes 1–6*). Homogenates from HEK-293A cells transiently cotransfected with cDNA templates encoding $P2X_4$-$(His)_6$ and either $P2X_1$-Flag, $P2X_4$-Flag, or $P2X_6$-Flag constructs were analyzed for copurification. After solid-phase binding of $P2X_4$-$(His)_6$ proteins on poly His-binding resin, we detected the coprecipitation of $P2X_4$-Flag subunits, confirming that $P2X_4$ subunits interacted between themselves to generate a homomultimeric complex (positive controls, Fig. 7*B*, *lane 1*). Coexpression of $P2X_4$-$(His)_6$ with $P2X_6$-Flag subunits gave a positive band corresponding to the expected size of $P2X_6$ (51 kDa; Fig. 7*B*, *lane 3*), demonstrating directly for the first time that $P2X_4$ and $P2X_6$ subunits do physically interact in a multimeric complex. Coexpression of $P2X_4$-$(His)_6$ with $P2X_1$-Flag subunits did not give any signal when probed with anti-Flag M2 antibodies after purification, confirming that $P2X_4$ and $P2X_1$ subunits do not heteropolymerize (Fig. 7*B*, *lane 5*). All control coexpressions including wild-type $P2X_4$ (lacking the poly-His motif) cotransfected with Flag-tagged $P2X_4$, $P2X_6$, or $P2X_1$ subunits were negative after purification on poly His-binding resin (Fig. 7*B*, *lanes 2, 4, 6*).

DISCUSSION

Functional identification of $P2X_{4+6}$ heteromeric receptors

In the present study, we first observed an apparent inhibition of $P2X_6$ subunits on ATP-induced currents in oocytes expressing $P2X_4$ subunits (Fig. 1*B*). However, neither ATP-induced currents

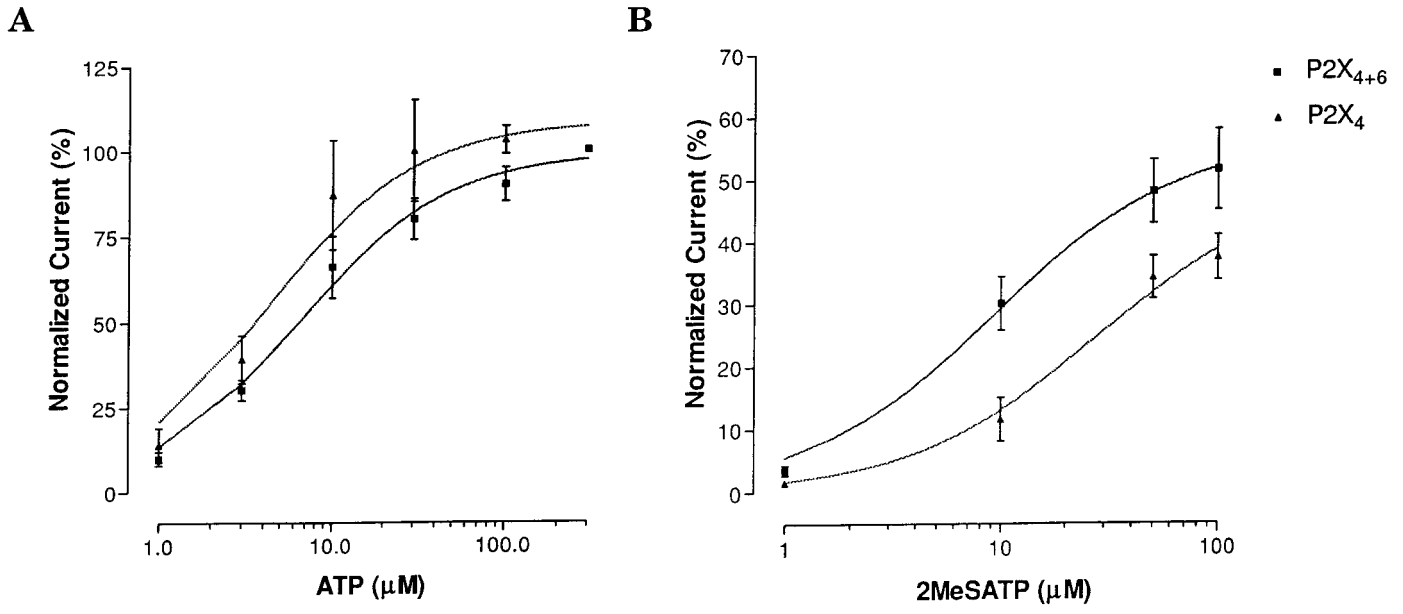

Figure 3. Sensitivity of $P2X_{4+6}$ receptors to the agonists ATP and 2MeSATP. *A*, Similar ATP dose–response profile between heteromeric $P2X_{4+6}$ channels and homomeric $P2X_4$ receptors in *Xenopus* oocytes. *B*, Heteromeric $P2X_{4+6}$ receptors showed increased sensitivity to 2MeSATP compared with $P2X_4$ receptors. Values are normalized to the response to 300 μM ATP (averages ± SEM from 3 to 7 oocytes per point in 2 independent experiments).

mediated by $P2X_1$ subunits (Fig. 1*C*) nor currents mediated by $P2X_2$ subunits (Fig. 1*D*) were affected, strongly suggesting that $P2X_4$ and $P2X_6$ isoforms associate together, in a subunit-specific manner, into a novel heteromeric P2X channel. Functional $P2X_{4+6}$ protein assembly and/or plasma membrane channel targeting appeared to be on a different time scale compared with $P2X_4$ receptors. Indeed, in response to 100 μM ATP, $P2X_{4+6}$ heteromultimers gave rise to increasing peak currents even after 5 d of expression (Fig. 2*A*), whereas $P2X_4$ homopolymers yielded decreasing peak current amplitudes under identical conditions (Fig. 2*B*). We did not find any difference between the EC_{50} values of ATP for both homomeric and heteromeric receptor isoforms (Fig. 4*A*), so we concluded that the apparent inhibitory effect of $P2X_6$ on $P2X_4$ recorded 3 d after injection was mainly attributed to a slower expression of $P2X_{4+6}$ receptors on the cell surface, assuming similar channel conductance. These findings constituted our first set of experimental evidence demonstrating a heteropolymerization between $P2X_4$ and $P2X_6$ subunits. It has been noticed previously that $P2X_6$ subunits and channels express poorly in HEK-293A cells (Collo et al., 1996) and are silent to ATP in the *Xenopus* oocyte expression system (Soto et al., 1996), as observed here. However, maximal ATP-induced peak currents were significantly larger at day 5 in the case of $P2X_{4+6}$ channels than in the case of $P2X_4$ alone (Fig. 2*A*). This situation is reminiscent of epithelial sodium-selective channels, belonging to another family of two-transmembrane-domain cation channels, whereby a fully functional channel requires the heteropolymerization of α subunits with β and γ subunits, both inactive when expressed alone (Canessa et al., 1994).

Unique pharmacological profile of $P2X_{4+6}$ heteromeric receptors

We made the assumption that the association between $P2X_4$ and $P2X_6$ subunits should be reflected in some unique aspects of the pharmacological profile of the resulting heteromeric receptor. Although $P2X_4$ seemed the dominant subunit for the sensitivity to ATP in the heteromers, we observed a statistical difference between EC_{50} values of 2MeSATP for $P2X_{4+6}$ heteromeric channels and $P2X_4$ receptors (Fig. 4*B*). Furthermore, in response to 100 μM $\alpha\beta$mATP applications, oocytes coexpressing $P2X_4$ and $P2X_6$ subunits gave rise to larger maximal peak currents than oocytes expressing $P2X_4$ isoforms alone (Fig. 3*A*), despite slower kinetics of expression. Indeed, we measured a lower EC_{50} of $\alpha\beta$mATP for $P2X_{4+6}$ than for $P2X_4$ channel species (Fig. 3*B*). Therefore, in addition to opposite protein expression profiles between $P2X_{4+6}$ and $P2X_4$ channels, these observations strongly indicate that $P2X_4$ and $P2X_6$ subunits generate a novel receptor phenotype characterized by a unique agonist profile, namely increased 2MeSATP and $\alpha\beta$mATP sensitivity. Moreover, these data provide for the first time experimental evidence for moderately desensitizing $\alpha\beta$mATP-activated ionotropic responses.

Furthermore, we probed the sensitivity of $P2X_{4+6}$ heteromers to P2 antagonists suramin, PPADS, and RB-2 coapplied with ATP. We found that suramin significantly blocked $P2X_{4+6}$ activity without inhibiting significantly $P2X_4$ homomeric receptors (Fig. 5*A*); 10 μM suramin coapplied with 100 μM ATP decreased $P2X_{4+6}$ heteromeric receptor peak current amplitudes by up to 40% compared with 7% for $P2X_4$ homomeric channels. Coapplied PPADS inhibited $P2X_{4+6}$ weakly, although it had no measurable effects on oocytes expressing $P2X_4$ subunits alone (Fig. 5*A*). After preincubation, low concentrations of RB-2 provided the most dramatic differential effect by inhibiting $P2X_{4+6}$ heteromers while potentiating $P2X_4$ channel activity (Fig. 5*B*). Suramin and RB-2 would thus be useful pharmacological tools to investigate the expression of native $P2X_{4+6}$ heteromers in $\alpha\beta$mATP-sensitive neuronal preparations.

Biochemical evidence of $P2X_{4+6}$ heteropolymers

We demonstrated direct interactions between the two predominant brain $P2X_4$ and $P2X_6$ isoforms through the use of an established copurification assay (Tinker et al., 1996). Based on our coprecipitation results with epitope-tagged subunits in nondenaturing conditions, $P2X_4$ associates with $P2X_6$ subunits (Fig. 7*B*). In *Xenopus* oocytes, this heteropolymerization underlies the spe-

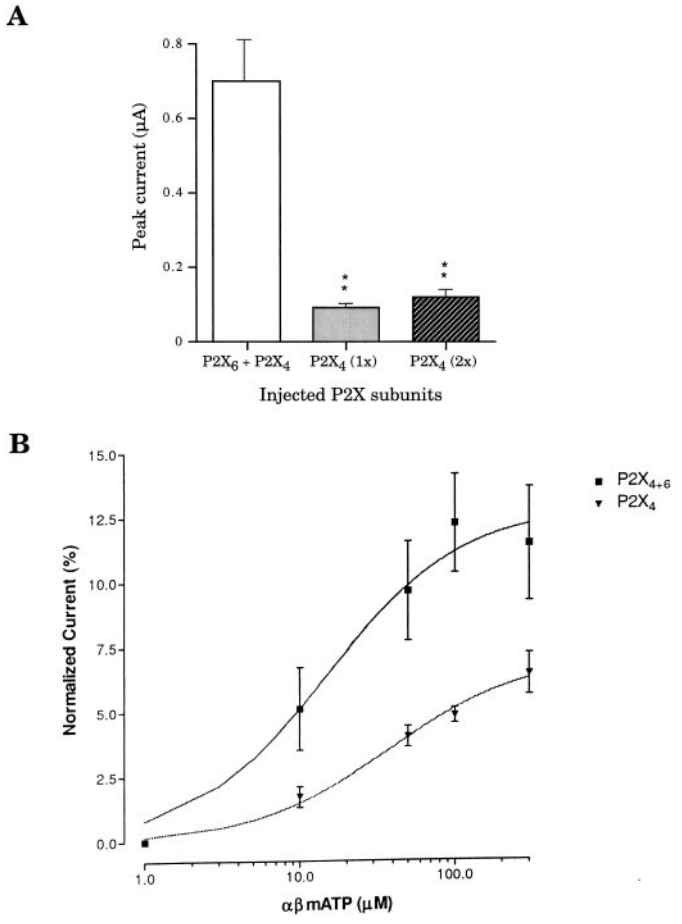

Figure 4. Sensitivity of $P2X_{4+6}$ receptors to the agonist $\alpha\beta$mATP. *A*, Differential $\alpha\beta$mATP responsiveness measured in peak current amplitudes between *Xenopus* oocytes expressing either $P2X_{4+6}$ channels or $P2X_4$ at day 3 after injection; see Figure 1*B* for comparison of ATP-induced peak currents. *B*, Normalized dose–response curves of $P2X_{4+6}$ and $P2X_4$ receptor species for $\alpha\beta$mATP. Values are normalized to the response to 100 μM ATP; *double asterisks* denote significant difference; $p < 0.01$ (averages ± SEM from 5 to 8 oocytes per point in 2 independent experiments).

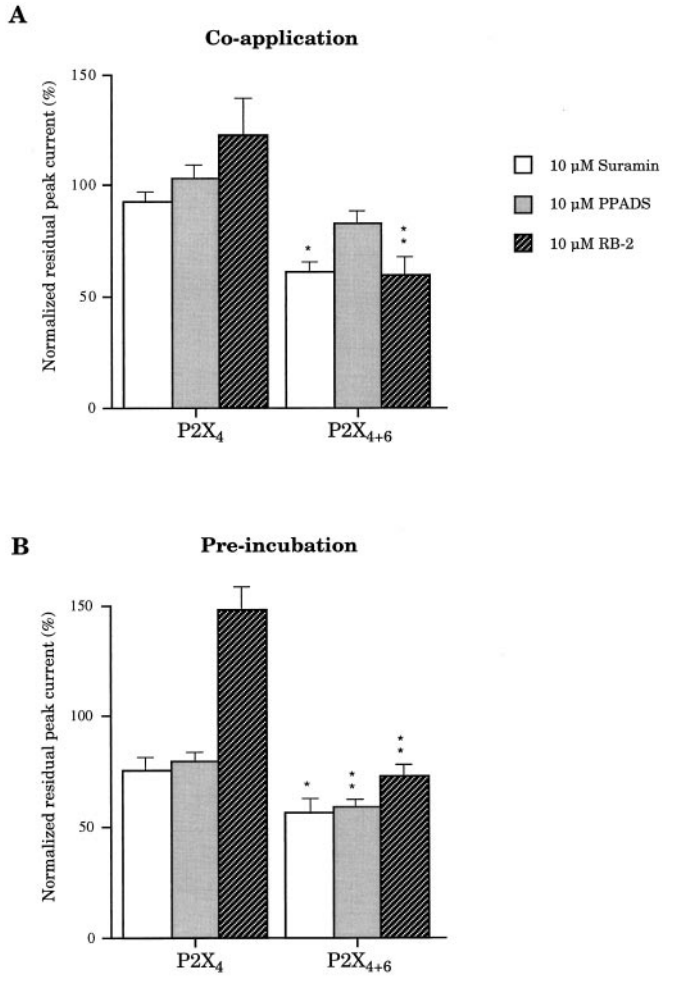

Figure 5. Sensitivity of $P2X_{4+6}$ to P2X antagonists. Suramin, PPADS, and RB-2 were tested for their blocking properties on heteromeric $P2X_{4+6}$ channels and on homomeric $P2X_4$ receptors. Antagonists were coapplied with ATP (*A*) or preincubated before coapplication (*B*). Note that $P2X_{4+6}$ receptors are inhibited, whereas $P2X_4$ receptors are potentiated by 10 μM RB-2. Values are normalized to the response to ATP only (averages ± SEM from 5 oocytes per experiment; *single* and *double asterisks* denote significant difference; $p < 0.05$ and $p < 0.01$, respectively).

cific pharmacological and electrophysiological phenotype of a novel heteromeric channel distinct from either $P2X_4$ or $P2X_6$ homomeric receptors. On the other hand, $P2X_4$ and $P2X_1$ subunits did not seem to interact significantly with each other (Fig. 7*B*). Furthermore, the absence of obvious phenotypical differences between oocytes coexpressing $P2X_6$ + $P2X_1$ and $P2X_1$ subunits alone (Fig. 1*C*), or between $P2X_6$ + $P2X_2$ and $P2X_2$ homomers (Fig. 1*D*), indicate that structural determinants of association between $P2X_4$ and $P2X_6$ isoforms are subunit-dependent. A similar biochemical approach using copurification of $P2X_4$ with chimeric subunits based on $P2X_6$ and $P2X_1$ structures could lead to the identification of the domain(s) involved in specific heteropolymerization.

Functional correlates of native $P2X_{4+6}$ heteromers

Purinergic responses from CA3 neurons in rat hippocampal slices have been shown recently to be activated by $\alpha\beta$mATP and inhibited by suramin but not by PPADS (Ross et al., 1998). Based on *in situ* hybridization results (Collo et al., 1996), $P2X_4$ and $P2X_6$ are the only P2X subunits expressed at significant levels in adult rat hippocampus, namely in CA1–CA4 hippocampal subfields

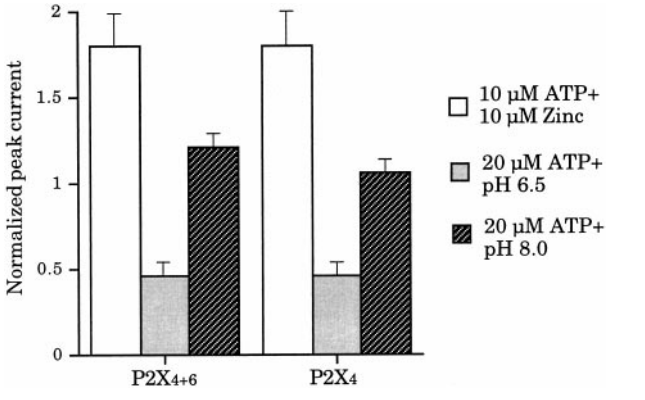

Figure 6. Sensitivity of $P2X_{4+6}$ to the extracellular cofactors zinc ions and pH. Extracellular Zn^{2+}, pH 6.5 and 8.0, coapplied with ATP, did not allow differentiation between $P2X_{4+6}$ and $P2X_4$ receptors. Values are normalized to the response to ATP only (averages ± SEM from 4 oocytes per experiment).

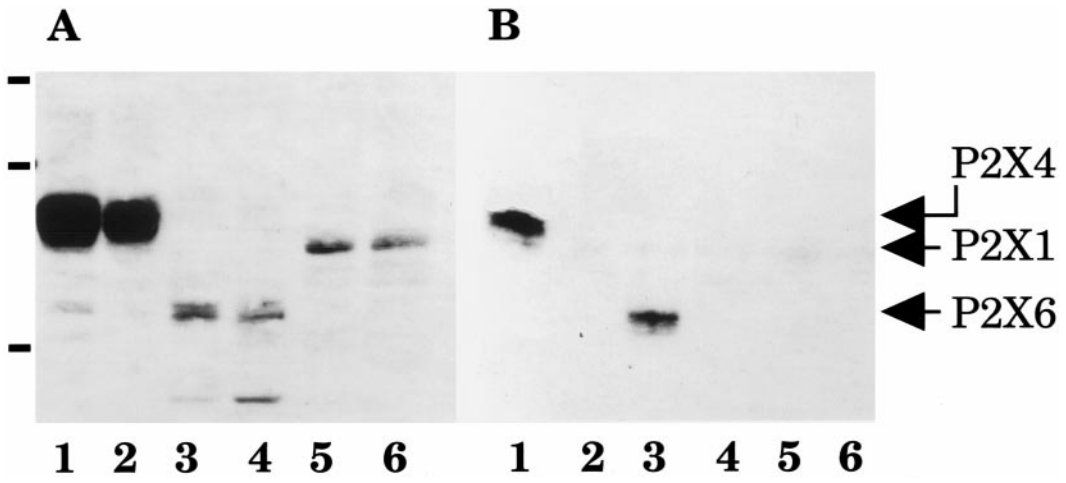

Figure 7. Subunit specificity of $P2X_4$ and $P2X_6$ heteropolymerization. *A*, Immunoblot of Flag-tagged $P2X_1$, $P2X_4$, and $P2X_6$ subunits probed with anti-Flag M2 monoclonal antibodies in total membrane proteins from transiently transfected HEK-293A cells. *B*, From the same samples, immunoblot of Flag-tagged $P2X_1$, $P2X_4$, and $P2X_6$ subunits probed with M2 antibodies after copurification through $P2X_4$-$(His)_6$ subunits. Molecular weight markers (in *A*): 104, 82, and 48 kDa. Cotransfections: *lane 1*, $P2X_4$-$(His)_6$ + $P2X_4$-Flag; *lane 2*, $P2X_4$-wt + $P2X_4$-Flag; *lane 3*, $P2X_4$-$(His)_6$ + $P2X_6$-Flag; *lane 4*, $P2X_4$-wt + $P2X_6$-Flag; *lane 5*, $P2X_4$-$(His)_6$ + $P2X_1$-Flag; *lane 6*, $P2X_4$-wt + $P2X_1$-Flag.

and in the dentate gyrus. Thus, our functional data obtained from recombinant receptors are in close agreement with this native phenotype and suggest that the sensitivities to $\alpha\beta$mATP and to suramin of rat CA3 neurons might be mediated through native $P2X_{4+6}$ heteromeric channels.

Neonatal rat cerebellar Purkinje cells have been characterized as having purinergic receptors with a $P2X_2$-like pharmacological profile in eliciting extracellular calcium influxes (Mateo et al., 1998). This conclusion rested on $\alpha\beta$mATP insensitivity, the potency ratio of ATP to 2MeSATP, as well as suramin and PPADS blockade after preincubation. However, on recombinant $P2X_{4+6}$ receptors, the concentration of $\alpha\beta$mATP used by Mateo et al. (1998) (50 μM) was ~10% as efficacious as 50 μM ATP in eliciting ionotropic responses, so $\alpha\beta$mATP-mediated intracellular calcium increases could have remained undetected and consequently interpreted as $\alpha\beta$mATP unresponsiveness. The developmental regulation of expression levels of neuronal P2X genes in cerebellum is not established so far. Adult rat Purkinje neurons are known to transcribe $P2X_4$ and $P2X_6$ mRNA (Collo et al., 1996) and have been shown to translate high levels of $P2X_4$ subunits (Lê et al., 1998), whereby $P2X_2$ mRNAs (Collo et al., 1996) or subunits (Vulchanova et al., 1996) were reported previously to be absent (Kanjhan et al., 1996). It is also possible that native P2X receptors in neonatal Purkinje cells are composed of three subunits, namely $P2X_2$, $P2X_4$, and $P2X_6$, assembled in a heteromeric complex in which $P2X_2$ is pharmacologically dominant. We have recorded in oocytes purinergic currents mediated by $P2X_{4+6}$ heteromeric channels that were significantly more sensitive to the agonists $\alpha\beta$mATP and 2MeSATP, as well as to the antagonist suramin compared with $P2X_4$ homomeric receptors. So it is likely that the moderately desensitizing $\alpha\beta$mATP-activated and suramin-sensitive postsynaptic purinergic responses recorded from medial habenula (Edwards et al., 1992) could be accounted for by the expression of postsynaptic $P2X_{4+6}$ receptors, because *in situ* hybridization results demonstrate the exclusive presence of $P2X_4$ and $P2X_6$ transcripts in this region (Collo et al., 1996). The widespread distribution of high-affinity [^{3}H]$\alpha\beta$mATP binding sites within the rat CNS (Bo and Burnstock, 1994; Michel and Humphrey, 1994; Balcar et al., 1995) appears to correlate with *in situ* hybridization data on $P2X_4$ and $P2X_6$ mRNA distributions (Collo et al., 1996; Séguéla et al., 1996) as well as with the immunocytochemical localization of $P2X_4$ protein (Lê et al., 1998). This neuroanatomical evidence strongly suggests that the $P2X_{4+6}$ channel phenotype might be present in most rat brain and spinal cord regions. Moreover, we have shown that the $P2X_4$ subunit is a major presynaptic purinoceptor component in laminae I and II of spinal cord and in olfactory glomeruli (Lê et al., 1998), two regions in which $P2X_6$ is also expressed (Collo et al., 1996). Therefore, the heteromeric $P2X_{4+6}$ ATP-gated cation channel could play a significant role in the regulation of excitatory transmitter release in central sensory synapses.

REFERENCES

Balcar VJ, Li Y, Killinger S, Bennett MR (1995) Autoradiography of P2X ATP receptors in the rat brain. Br J Pharmacol 115:302–306.

Bo X, Burnstock G (1994) Distribution of [^{3}H]α,β-methylene ATP binding sites in rat brain and spinal cord. NeuroReport 5:1601–1604.

Bo X, Zhang Y, Nassar M, Burnstock G, Schoepfer R (1995) A P2X purinoceptor cDNA conferring a novel pharmacological profile. FEBS Lett 375:129–133.

Brake AJ, Wagenbach MJ, Julius D (1994) New structural motif for ligand-gated ion channels defined by an ionotropic ATP receptor. Nature 371:519–523.

Buell G, Collo G, Rassendren F (1996) P2X receptors: an emerging channel family. Eur J Neurosci 8:2221–2228.

Canessa CM, Schild L, Buell G, Thorens B, Gautschi I, Horisberger J-D, Rossier BC (1994) Amiloride-sensitive epithelial Na^+ channel is made of three homologous subunits. Nature 367:463–467.

Chen C-C, Akopian AN, Sivilotti L, Colquhoun D, Burnstock G, Wood JN (1995) A P2X purinoceptor expressed by a subset of sensory neurons. Nature 377:428–431.

Collo G, North RA, Kawashima E, Merlo-Pich E, Neidhart S, Surprenant A, Buell G (1996) Cloning of $P2X_5$ and $P2X_6$ receptors and the distribution and properties of an extended family of ATP-gated ion channels. J Neurosci 16:2495–2507.

Edwards FA, Gibb AJ, Colquhoun D (1992) ATP receptor-mediated synaptic currents in the CNS. Nature 359:144–147.

Kanjhan R, Housley GD, Thorne PR, Christie DL, Palmer DJ, Luo L, Ryan AF (1996) Localization of ATP-gated ion channels in cerebellum using $P2X_{2R}$ subunit-specific antisera. NeuroReport 7:2665–2669.

Khakh BS, Humphrey PPA, Surprenant A (1995) Electrophysiological properties of P2X-purinoceptors in rat superior cervical, nodose, and guinea pig coeliac neurones. J Physiol (Lond) 484:385–395.

Lê K-T, Villeneuve P, Ramjaun AR, McPherson PS, Beaudet A, Séguéla P (1998) Sensory presynaptic and widespread somatodendritic immunolocalization of central ionotropic P2X ATP receptors. Neuroscience 83:177–190.

Lewis C, Neidhart S, Holy C, North RA, Buell G, Surprenant A (1995) Coexpression of $P2_X2$ and $P2X_3$ receptor subunits can account for ATP-gated currents in sensory neurons. Nature 377:432–435.

Mateo J, Garcia-Lecea M, Miras-Portugal MT, Castro E (1998) Ca^{2+} signals mediated by P2X-type purinoceptors in cultured cerebellar Purkinje cells. J Neurosci 18:1704–1712.

Michel AD, Humphrey PPA (1994) Distribution and characterization of [^{3}H]α,β-methylene ATP binding sites in the rat. Naunyn- Schmiedebergs Arch Pharmacol 348:608–617.

North RA, Barnard EA (1997) Nucleotide receptors. Curr Opin Neurobiol 7:346–357.

Radford KM, Virginio C, Surprenant A, North RA, Kawashima E (1997) Baculovirus expression provides direct evidence for heteromeric assembly of $P2X_2$ and $P2X_3$ receptors. J Neurosci 17:6529–6533.

Ross FM, Brodie MJ, Stone TW (1998) Modulation by adenine nucleotides of epileptiform activity in the CA3 region of rat hippocampal slices. Br J Pharmacol 123:71–80.

Séguéla P, Haghighi A, Soghomonian JJ, Cooper E (1996) A novel neuronal P2X ATP receptor ion channel with widespread distribution in the brain. J Neurosci 16:448–455.

Soto F, Garcia-Guzman M, Karschin C, Stühmer W (1996) Cloning and tissue distribution of a novel P2X receptor from rat brain. Biochem Biophys Res Commun 223:456–460.

Stoop R, Surprenant A, North RA (1997) Differential sensitivities to pH of ATP-induced currents at four cloned P2X receptors. J Neurophysiol 78:1837–1840.

Tinker A, Jan YN, Jan LY (1996) Regions responsible for the assembly of inwardly rectifying potassium channels. Cell 87:857–868.

Valera S, Hussy N, Evans RJ, Adami N, North RA, Surprenant A, Buell G (1994) A new class of ligand-gated ion channel defined by P2X receptor for extracellular ATP. Nature 371:516–519.

Vulchanova L, Arvidsson U, Riedl M, Wang J, Buell G, Surprenant A, North RA, Elde R (1996) Differential distribution of two ATP-gated ion channels (P2X receptors) determined by immunocytochemistry. Proc Natl Acad Sci USA 93:8063–8067.